Engineered Disulfide Bonds Restore Chaperone-like Function of DJ-1 Mutants Linked to Familial Parkinson's Disease

ARTICLE *in* BIOCHEMISTRY · JULY 2010

Impact Factor: 3.02 · DOI: 10.1021/bi902164h · Source: PubMed

3 AUTHORS, INCLUDING:

Todd Logan
University of California, San Francisco
5 PUBLICATIONS **226** CITATIONS
SEE PROFILE

Soumya S Ray
Brigham and Women's Hospital
23 PUBLICATIONS **598** CITATIONS
SEE PROFILE

Published in final edited form as:
Biochemistry. 2010 July 13; 49(27): 5624–5633. doi:10.1021/bi902164h.

Engineered disulfide bonds restores chaperone like function of DJ-1 mutants linked to familial Parkinson's disease

Todd Logan[#,*], **Lindsay Clark**[#,@], and **Soumya S. Ray**[#,*,&,@]

[@]Harvard Center for Neurodegeneration and Repair and Department of Neurology, Harvard Medical School.

[#]Center for Neurologic Diseases, Brigham and Women's Hospital.

Abstract

Loss-of-function mutations such as L166P, A104T and M26I in the DJ-1 gene (PARK7) have been linked to autosomal-recessive early onset Parkinson's disease (PD). Cellular and structural studies of the familial mutants suggest that these mutations may destabilize the dimeric structure. In order to look for common dynamical signatures among the DJ-1 mutants, short MD simulations up to 1000ps were carried out to identify the weakest region of the protein (residues 38–70). In an attempt at stabilizing the protein, we mutated residue Val 51 to cysteine (V51C) to make a symmetry-related disulfide bridge with the pre-existing Cys 53 on the opposite subunit. We found that the introduction of this disulfide linkage stabilized the mutants A104T and M26I against thermal denaturation, showed increased ability to scavenge reactive oxygen species (ROS) and restored a chaperone-like function of blocking α-synuclein aggregation. The L166P mutant was far too unstable to be rescued by introduction of V51C. The results presented here points towards the possible development of pharmacological chaperones, which may eventually lead to PD therapeutics.

Parkinson's Disease is a progressive neurodegenerative disease characterized by the loss of dopaminergic neurons from the substantia nigra *pars compacta*, and the presence of cytosolic inclusions known as Lewy bodies (1). These inclusions are rich in fibrils of α-synuclein and parkin. A more recently identified gene product of unknown function, DJ-1 (PARK7, location 1p36.2-3 on the human genome), has been implicated in autosomal-recessive early onset PD(2). Mutations in the DJ-1 gene include a 14kb deletion encompassing the first six exons(2), as well as missense mutations encoding DJ-1 variants. L166P, one of the well studied variants appears to cause dramatic loss of stability leading to low cellular levels of protein (3,4). Other variants such M26I(5,), E64D(6) and E163K(7) are also known to affect cellular levels of DJ-1 but to lesser extent compared to L166P. These homozygous mutations may trigger a loss-of-function, the presumed cause of their pathogenicity. Another variant A104T(8,9) was associated PD patients in heterozygous state and structural analysis of the x-ray structure reveals local perturbations in the central β-sheet suggesting that mutation may lead to loss of stability(10). Apart from the association of DJ-1 with recessive Parkinson's disease, DJ-1 has been implicated in pathogenesis of various

---

[&]Address: 65 Landsdowne St., #452, Cambridge, MA 02139, address correspondence to sray@rics.bwh.harvard.edu, ph: +1-617-821-0955, Fax: +1-617-768-8606.
[*]These authors have equal contribution in this manuscript

Availability of supplementary material:
Supplementary material for this article is available immediately for download free of charge from http://www.acs.org . The supplementary material includes a ribbon diagram color coded by the motion observed in our simulation studies, control experiments with reduced forms of the disulfide bonded double mutants of DJ-1 and SDS-PAGE analysis of disulfide bonded DJ-1^{V51C} and α-synuclein mixtures.

types of cancer(11), may play a role in male fertility(12) and may reduce oxidative stress following stroke(13). Although the exact biochemical function of DJ-1 is not known, it has been shown to associate with transcription factors (14–17), bind RNA (18) and undergo SUMOylation(19). Furthermore, DJ-1 may have an overall effect on cell fate through its involvement in the PTEN/Akt signaling pathway(20). Wild-type DJ-1 has been shown to rescue α-synuclein aggregation *in vitro* pointing towards a possible chaperone like function(21–23). We demonstrate in this manuscript that the mutations that lead to structural defects in DJ-1 may be restored to near wild-type-like stability and function by covalently reinforcing the weak parts of the protein with appropriately placed disulfide bridges.

DJ-1 is a dimeric member of the ThiJ/Php family of proteins with an α/β fold homologous to the flavodoxin-like molecular chaperone Hsp31(24,25). The oxidation of a key highly conserved residue, C106, results in an acidic PI shift, which may signal DJ-1 to translocate to the mitochondria(26). The translocation to mitochondria is believed to be neuroprotective in nature(27). It has been suggested that translocation of DJ-1 to the mitochondria may play an important role in mitochondrial autophagy(28), an important cellular process known to be compromised in age-related disorders such as PD(29,30). Cys 106 is surrounded by charged amino acids from both subunits of the protein generating a unique chemical environment, suggesting the importance of a dimeric quaternary structure for normal protein function(31,32). In contrast to wild-type DJ-1, the PD-linked mutant L166P is highly destabilized, as judged by *in vitro* studies (33), the yeast two-hybrid system (4) and mammalian cells(34). While L166P causes severe structural defects, M26I was reported to be less stable WT and produce lower steady state levels in cell culture studies(35). Reduced dimer population was observed for A104T in cross-linking studies in cell culture systems but not in co-immunoprecipitation assays(36). X-ray crystallographic analysis indicates loss of stability for M26I, A104T and E163K (10) but they appear to retain dimeric structure in solution. M26I disrupts the hydrophobic core, A104T causes packing defects in a critical β-sheet near the C-terminus and E163K disrupts a structurally critical salt-bridge.

The central hypothesis of this manuscript is based on the notion that if the ‘weakest structural link’ in a mutant protein structure can be identified, it may be reinforced with either covalent bond, such as disulfide linkages, or with small molecules to prevent the subsequent downstream unfolding events. This strategy has been successfully applied to transthyretin (involved in familial amyloid polyneuropathy)(37) and SOD-1 (involved in ALS)(38), where simple stabilization of the native dimeric (SOD) or tetrameric (TTR) states with small molecules or disulfide bridges abolished aggregation(37,39). A 1000psec MD simulation of L166P, M26I and A104T revealed that the region of the protein from residues 38–70 exhibited the most variation in motion when compared to the WT DJ-1. This region was also observed to have high degree of motion in experimental methods such as NMR carried out by Eliezer and co-workers (40) and in X-ray crystallographic solvent-mapping analysis by Ringer and co-workers(41). Simulation studies carried out on L166P by Daggett and co-workers have also indicated this same region to be disrupted early in the simulation(42). In this manuscript, we demonstrate covalently reinforcing the dimer interface region with disulfide bonds can lead to increased protein stability, improved antioxidant function of the mutant protein and promoted chaperone like function in DJ-1 mutants. Though, familial DJ-1 mutations represent a small class of PD causing mutation, promoting or prolonging anti-aggregation function of WT DJ-1 might help patients with various synucleinopathies.

Materials and methods

Protein Expression and purification

Rosetta competent cells (Novagen) were transformed with pGEX GST fusion vectors (GE Healthcare) encoding wild-type DJ-1, as well as DJ-1^{L166P}, DJ- 1^{M26I}, DJ-1^{V51C}, DJ-$1^{L166P/V51C}$, DJ-$1^{M26I/V51C}$ and DJ-$1^{V51C/A104T}$ variants of DJ-1 genes synthesized by DNA2.0 (https://www.dna20.com/) with codons optimized for expression in *E. coli*. Cells were grown at 37°C in LB broth containing 100μg/ml ampicillin and 50μg/ml chloramphenicol until an OD_{600} of 0.4. Protein expression was initiated by addition of 750μM isopropyl-β-D-thiogalactopyranoside (IPTG) followed by incubation at 18°C for 16 h. Cells were harvested by centrifugation and stored at −80°C. Frozen cells resuspended in phosphate buffered saline (PBS), pH 7.4/ 400mM KCl were lysed using a Microfluidizer (Microfluidics Corporation) and centrifuged at 20000 × g for 45 min. Supernatant was loaded using a peristaltic pump to a GSTPrep FF16/10 column (GE Healthcare) that had been pre-equilibrated with 3 column volumes of PBS pH 7.4 / 400mM KCl. The GST column was washed with ~100mL of PBS/400mM KCl and protein was eluted with a solution containing 250mM Tris-HCl, pH 7.4/1.25M NaCl/10mM reduced L-glutathione. Eluate was combined with 500u Prescission Protease (GE Healthcare) and dialyzed overnight against PBS pH 7.4/400mM KCl/ 1mM DTT to cleave the GST-tag. The GST-tag was subtracted by flowing the cut protein back over the same column. Flow-through fractions were analyzed by SDS-PAGE and concentrated using Centiprep YM-10 centrifugal filter devices (Amicon) to a final volume of ~ 10mL, and further purified by size exclusion chromatrography on a Superdex 75 gel filtration column (GE Healthcare). Collected fractions were analyzed by SDS-PAGE and adjusted to a final concentration of ~ 4mg/ml. The protein samples were dialyzed extensively against 50mM tris pH 8.0 buffer with a minimum of three buffer changes. The extensive dialysis induced disulfide bond formation in DJ-1^{V51C}, DJ-$1^{L166P/V51C}$, DJ-$1^{M26I/V51C}$ and DJ-$1^{V51C/A104T}$ variants by air oxidation but not oxidation of C106 as judged by mass spectrometric analysis. Complete oxidation of Cys 106 was induced by incubating the protein with 0.1% H_2O_2 for one hour prior to its use in the α-synuclein aggregation assay but not for the glutathione peroxidase assay (described below). MALDI mass spectrometry was carried out to determine accurate molecular masses as well as assess the oxidation state of Cys 106.

Molecular dynamics simulation

The initial protein structures for DJ-1^{WT} (1pdv), DJ-1^{M26I} (2rk4) and DJ-1^{A104T} (2rk3) were downloaded from the protein databank (http://www.rcsb.org/pdb) and examined to add all the missing side chains to generate a model suitable for simulation studies. The familial DJ-1 mutations L166P (no structure available) was modeled using PYMOL. Following addition of hydrogen at all the relevant positions, the resulting structures were energy minimized to remove any geometric strains that might have been introduced as a result of the modeling procedure. His residues were protonated at Nδ2 except His-138 was protonated at Nδ1. Tautomer assignments for His residues were based on investigation of likely hydrogen bonds in the crystal structure. GROMACS ver3.2(43) using the GROMOS96 forcefield was chosen for all the subsequent steps in the simulation procedure. The protein structures were enclosed in a cubic box and filled with water molecules such that the waters extended 5Å from the protein molecule. Energy calculations were carried out using periodic boundary conditions and the calculation of electrostatic energy were carried out using particle mesh Ewald (PME) summations and a non-bonded cutoff at 10Å. The simulation overall involved five major steps (1) Energy minimization of the system in 500 steps of the steepest decent followed by 500 steps of conjugate gradient energy minimization at a constant volume. (2) Restrained molecular dynamics for 10ps at 300°K while freezing the position of the protein and the ions and moving only the solvent. (3) 10 psec of warming

the whole system to 300°K at constant volume using new, random velocities; and (4) 1 nsec MD of the whole system at a constant temperature of 500°K and constant pressure of 1 atmosphere after pre-warming of the system to 700°K for 20 ps. The generation of a control trajectory at 300°K for WT DJ-1 was carried out in a similar fashion. Snapshots of the structures were saved every 2 psec during the trajectories. The simulations were undertaken on a Beowulf cluster using eight node 3.0GHz Xeon processors configured in dual processor nodes (16 CPU total). The resulting coordinates were analyzed using the program G_RMSF from the GROMACS(43) software suite.

Glutathione peroxidase assay for DJ-1 autooxidation

A Glutathione Peroxidase Assay Kit (Cayman Chemical) was used to measure peroxidase activity of DJ-1. Protein samples were diluted to 100μM final concentration in assay buffer (50mM Tris-HCl pH 7.6 / 5mM EDTA) and a substrate mixture containing NADPH, glutathione, and glutathione reductase. Reactions were initiated by addition of cumene hydroperoxide, and absorbance was monitored at 340nm using a SpectraMax Plus plate reader (Molecular Devices). All samples were normalized to the activity of a glutathione peroxidase (100nM) positive control (provided by Cayman chemicals). Data points were averaged over five independent experimental measurements.

Differential scanning fluorimetry using Thermofluor®

Solutions of 7.5 μl of 100X Sypro Orange (Invitrogen) and 10μM protein were added to the wells of a 96-well thin-wall PCR plate (Bio-Rad). The plates were sealed with Optical-Quality Sealing Tape (Bio-Rad) and heated in an iCycler iQ5 Real Time PCR Detection System (Bio-Rad) from 4 to 90 °C in increments of 0.5 °C. Fluorescence changes in the wells of the plate were monitored simultaneously with a charge-coupled device (CCD) camera. The wavelengths for excitation and emission were 490 and 575 nm, respectively. For each protein sample, data from three independent wells were averaged and plotted.

α-synuclein fibrillation Assay

Fibril formation was monitored using a ThioT assay. Samples of α-synuclein were dissolved in 50mM Tris-HCl (pH 8.0) and filtered through a Millipore Microcon 100K MWCO filter. The final concentration in the reaction mixture was adjusted to 75μM. 75μM amounts of DJ-1^{WT} or the mutants (preincubated with 0.1% H_2O_2) were added to α-synuclein and pre-incubated over ice for 30min prior to aggregation. In cases of control experiments, where the effect of reducing the disulfide bond in DJ-$1^{M26I/V51C}$ and DJ-$1^{V51C/A104T}$ on α-synuclein aggregation was explored, the protein right after purification was dialyzed overnight with 10mM DTT to ensure all cysteine residues were in free thiol form. Mass spectrometric analysis revealed that Cys 106 was in thiol form in these protein samples. Aggregation was initiated by incubating the samples at 37 °C with constant stirring with a ministirring bar. 10μl samples of the aggregating mixture were withdrawn at regular intervals and assayed for fibril content by monitoring ThioT fluorescence. Data from five independent aggregation assays for α-synuclein incubated various forms of DJ-1 was used for generation of the data plot and error bars. Thio-T, (Sigma) was filtered through a 0.2-μm polyether sulfone filter and added to the sample wells (384 well format plate) at a final concentration of 20μM and incubated for 1 min prior to recording of fluorescence. Samples were mixed by agitation for 60sec at 120rpm. Fluorescence enhancement was monitored at 490nm by an Analyst 96–384 plate reader (LJL Biosystems).

Electron microscopy analysis

Samples of α-synuclein, DJ-1 and mixtures of a-synuclein and DJ-1 were diluted 6-fold with TBS prior to adsorption to glow-discharged, carbon-coated copper grids. Grids were washed

with four drops of buffer and stained with two drops of freshly prepared 0.75% (w/v) uranyl formate (Pfaltz & Bauer, Waterbury, CT 06708). Specimens were inspected with a JEOL 1200EX - 80kV electron microscope operated at 80 kV, and images were taken at a nominal magnification of 40000 using low-dose procedures.

Analytical size exclusion chromatography

All chromatography was performed in TBS (20 mM Tris, 150 mM NaCl), pH 7.4, on a Waters 2690 Alliance HPLC or Agilent 1100 series HPLC and monitored at 276 nm. Protein samples were spun at 13,000g prior to injection on the column.

Results

Structural changes in the familial mutants DJ-1^{L166P}, DJ-1^{A104T} and DJ-1^{M26I} probed by MD simulation

Familial DJ-1 mutants are distributed all over various secondary structural elements on the protein structure (Figure 1a) and appear to have a wide range of effect on protein folding and stability. The central hypothesis behind this investigation is based on the notion that covalent tethering of protein residues using disulfide bonds in the most facile region should be able to improve overall stability of the mutant and possibly restore wild-type like function (44–46). It was therefore useful to carry out MD simulations of the various DJ-1 mutants and compare them with each other and DJ-1^{WT} in order to look for a common dynamical signature. Daggett and co-workers (42) have carried out simulation studies on DJ-1^{L166P} and shown destabilization near the dimer interface regions. In this section, we have extended the studies to other familial DJ-1 mutants to Parkinson's disease. Short molecular dynamic simulations were carried out on DJ-1WT(1pdv), DJ-1^{M26I}(1rk4) and DJ-1^{A104T}(1rk3) at 700K using the program GROMACS (43) for a total of 1000ps (1ns) in the presence of water molecules. Since there is no crystal structure for L166P, the mutation was modeled into DJ-1^{WT}(1pdv) and simulated under the conditions described above. The Cα atom root mean square deviation (RMSD) from the crystal structure was calculated for all of the snapshots from each residue to give an approximate idea of the degree of structural perturbation during the course of the simulation (Figure 2a). The control trajectory for WT DJ-1 at 300K shows less than 1.5Å deviation from the initial crystal structure suggesting that the system remains stable at room temperature. The familial mutants, DJ-1^{L166P}, DJ-1^{A104T} and DJ-1^{M26I} when simulated at 700K showed increased mobility and perturbation from the initial model. The mutants DJ-1^{L166P}, DJ-1^{A104T} showed greater degree of perturbation compared to DJ-1^{M26I} under identical simulation conditions. The majority of the RMSD from the initial structure could be accounted for by motions around the N and C-termini of the protein, the regions 38–70 and 127–138 (Figure 2a). The solvent exposed helix 6 between residues 127–138 shows the highest degree of perturbation from the initial structures and appears to be the most mobile region of the protein. Though this region shows high R.M.S.D, it appears to be a common region of high mobility between the WT and the mutants. This is therefore likely to be a natural protein motion and not induced by entirely by mutation. It is currently not possible to deduce the precise origin of this motion from the short simulation studies. Similar observations of natural protein motions *vs* mutation induced motions have been made in simulation studies carried out on other protein systems(47).

The region 38–70 in the control trajectory (WT at 300K) and WT at 700K exhibited less motion when compared to the familial mutants. When the motion was mapped on the crystal structures of M26I, A104T and the L166P model, this region of highest perturbation coincided with parts of the dimer interface of DJ-1 (Figure 2b shown for DJ-1^{A104T}) near the β3 and β4 strand regions. Large motion was also observed in helix B (numbering scheme

adapted from reference (48)). Among the three mutants, M26I showed the least amount of motion relative to the WT protein around residues 38–70. It is noteworthy that this region is located roughly 21Å from the A104T mutation site, 17Å from M26I and 25Å from L166P, suggesting long range coupling between the mutation site and the region 38–70 (Figure 2a and supplementary figure 1a). Similar observations have been made in the case of other proteins as well (47). The motion in the Cys 106 region does not appear to be much different between WT and the mutants in this short simulation study. However, we cannot rule out larger motions in this region in longer simulation studies.

Inter-subunit disulfide bonds in the facile region stabilize familial PD-linked mutant DJ-1 against thermal denaturation

Though a detailed analysis of the simulation trajectory has not been carried out in this study, preliminary analysis suggests that the 38–70 region of mutant DJ-1 is one of the most facile regions (maximum R.M.S.D). It may be hypothesized that covalently reinforcing this region using disulfide bridges should lead to overall stabilization of the protein. Based on DSDESIGN(49) disulfide modeling, it was concluded that the mutation V51→C51 (V51C) would result in a pair of symmetry related disulfide bridges with C53 on the opposite subunit with near optimal stereochemistry (Figure 1a). Mere proximity of cysteine residues is not sufficient to induce disulfide bond formation (stereochemical parameters are critical(49), see table in figure 1). The V51C mutation was introduced into the L166P, M26I and A104T familial DJ-1 variants. The double mutants DJ-$1^{A104T/V51C}$, DJ-$1^{L166P/V51C}$ DJ-$1^{M26I/V51C}$ and DJ-1^{V51C} were purified, and following air oxidation to generate the disulfide bridges between the native cysteine (C53) and the introduced cysteine (V51C), the protein samples were analyzed on SDS-PAGE under non-reducing conditions (Figure 1b). In contrast to protein harboring the familial mutations alone, the oxidized versions of the double mutants bearing the V51C mutation migrated as a ~42KDa band (Figure 1b; greater than 90% of the protein migrated as dimer) indicating that the engineered cysteine residues resulted in a covalently cross-linked dimeric form of DJ-1. DJ-$1^{L166P/V51C}$ mutant failed to migrate as a dimer in our SDS-PAGE analysis. This finding is in agreement with its being an extreme destabilizing mutation probably leading to loss of quaternary and tertiary protein structure.

Following oxidation, the thermal stability of the various mutants was measured using ThermoFluor® (differential scanning fluorimetry) on a PCR machine with real-time optics (details in materials and method section) (50–52). Briefly, the protein samples were gradually heated from 25°C to 80°C in increments of 0.5°C, and fluorescence from sypro-orange was measured (emission = 570nm). Sypro orange (ThermoFluor®) has low quantum yield in aqueous solution but readily binds to unfolding proteins with almost 1000 fold increase in quantum yields and, therefore, is an ideal probe for monitoring the thermal stability of a protein. Thermal melting profiles were measured from three independent PCR wells (n=3) for each sample. DJ-1^{WT} was found to be most stable with Tm=65±0.5°C (Figure 1c). The familial mutants were found to be less stable than WT with DJ-1^{M26I} (Tm=52±0.5°C) and DJ-1^{A104T}(Tm=53±0.5°C) respectively. Compared to the familial PD mutants alone, the V51C disulfide-linked versions of the mutant DJ-1 exhibited higher degree of thermostability (DJ-$1^{M26I/V51C}$ Tm=57±0.5°C, DJ-$1^{A104T/V51C}$ Tm=58±0.5°C) (Figure 1c). Thermal stabilization upon introduction of disulfide bonds to similar degrees have been reported for other protein systems as well (53–55).

Disulfide linkages restore antioxidant like function in DJ-1 harboring familial mutations

Since the disulfide linkages could effectively stabilize mutant DJ-1, we attempted to demonstrate that this would also lead to restoration of a ‘protein function’ (the real function of DJ-1 is not known) that is contingent on protein stability. As mentioned earlier, a highly

reactive cysteine (Cys 106) residue is in close proximity to Glu 18, His 126 and Arg 28 and located in a unique chemical environment made up by residues from both subunits(32). This structural feature gives DJ-1 the ability to reduce reactive oxygen species (ROS) by undergoing self-oxidation at Cys 106 to generate a cysteine sulfenic acid (31). This reaction is similar in mechanism to that utilized by the glutathione peroxidase class of enzyme. However, unlike glutathione peroxidase, it appears to be a stoichiometric, rather than a catalytic, reaction. To assess the ability of the various familial DJ-1 mutants to reduce ROS (in this case, cumene hydroperoxide), we employed a spectrophotometric assay that takes advantage of the observed decrease in NADPH absorbance that accompanies the glutathione oxidation-reduction reaction. In our assay, the observed decrease in NADPH absorbance is directly proportional to the peroxidase activity of the sample. DJ-1 self oxidation is not catalytic bur rather stoichiometric nature. The various DJ-1 samples were adjusted to a concentration of 100uM (the high concentration necessary for DJ-1^{WT} to exhibit activity comparable to the glutathione peroxidase control of 100nM), incubated with a co-substrate mixture and the absorbance monitored at 340nm for 30 min. Stoichiometric self oxidation of DJ-1^{WT} and the various mutants were measured in five independent experiments (n=5) and averaged data is shown in figure 3a. Our results show that the familial mutations DJ-1^{A104T} and DJ-1^{M26I} display a deficit in their capacity to reduce cumene hydroperoxide (Figure 3a). In contrast, their disulfide-linked mutants DJ-$1^{A104T/V51C}$ and DJ-$1^{M26I/V51C}$ were more effective in scavenging ROS in the above-mentioned assay compared to their familial mutant counterparts. This demonstrates that the stabilization of the mutants using disulfide bridges restores local structure near Cys 106 necessary for scavenging ROS.

Disulfide linkages rescue DJ-1s ability to inhibit α-synuclein aggregation

Wild type DJ-1 has been shown to suppress aggregation of α-synuclein suggesting a possible chaperone like function for DJ-1(21–23). This property is highly dependent on the oxidation state of DJ-1, particularly that of Cys 106(10). If this is indeed true, the loss of stability in this region in the L166P, A104T and M26I familial mutants should lead to deficits in their ability to inhibit α-synuclein fibrillization. To test this hypothesis, we measured aggregation rates for α-synuclein in the presence of the familial mutants DJ-1^{A104T} and DJ-1^{M26I}. Fibrillization of α-synuclein induced by agitation was measured by monitoring the increase in thioflavin-T fluorescence at 490nm (details in materials and method section). Under agitation, samples of α-synuclein aggregated to completion in 48 hrs (Figure 3b). Wild-type DJ-1, added to the α-synuclein sample in equimolar quantities, slowed down α-synuclein aggregation, which was in good agreement with previously published data(23). No aggregation of α-synuclein in presence of DJ-1^{WT} was observed within 48 hrs but the samples starts to produce thio-T positive aggregates after 80 hrs (Figure 3b). The implications of this result are discussed in further details in the later sections. The addition of A104T or M26I mutant DJ-1 had no effect on the kinetics of α-synuclein aggregation. However, when introduced in equimolar concentrations to α-synuclein, oxidized samples of the double mutants DJ-$1^{A104T/V51C}$ and DJ-$1^{M26I/V51C}$ blocked the aggregation beyond 48 hours but not beyond 80 hours (Figure 3b). This is strong evidence that the chaperone-like function of DJ-1 is dependent on protein stability and possibly oxidation of Cys 106. Control experiments were carried out with the reduced form of both DJ-$1^{M26I/V51C}$ and DJ-$1^{A104T/V51C}$ generated right after purification by extensive dialysis with 10mM DTT. The assay conditions were identical to the one described above. The reduced form of DJ-$1^{A104T/V51C}$ and DJ-$1^{M26I/V51C}$ did not block aggregation of α-synuclein indicating that effect is not the mere presence of the V51C mutation but rather dependent on formation of the disulfide bond (Figure 1b supplemental information).

Disulfide linked wild-type DJ-1 has enhanced ability to block aggregation of α-synuclien

The presence of a disulfide bond restores chaperone like properties in the familial mutants. However, familial DJ-1mutants represents a fairly small group in the PD patient population. On the other hand, several lines of evidence point towards a central role for the process of α-synuclein fibrillization in the etiology of PD(56,57). If wild type DJ-1 is a natural chaperone for α-synuclien, stabilization of the WT protein should lead to enhancement of its anti-aggregation properties. In order to test this, we carried our prolonged aggregation assays (beyond 80 hours) with α-synuclien in presence of DJ-1^{WT} and DJ-1^{V51C} (Figure 3b and Figure 4a). Fibrillization of α-synuclein was induced by agitation in a manner similar to our previous experiments and was measured by monitoring the increase in thioflavin-T fluorescence at 490nm (details in materials and method section). Under agitation, samples of α-synuclein aggregated to completion under 48 hrs (Figure 4a). In presence of DJ-1^{WT}, no aggregation was observed until 80 hrs, following which there was rapid onset of α-synuclein aggregation(Figure 3b and Figure 4a). In presence of DJ-1^{V51C}, no aggregation was observed until 196hrs beyond which no further data points were collected. Samples containing DJ-1^{WT} and α-synuclein mixtures upon electron microscopy analysis (Figure 4b) at 80 hrs into the assay were found to contain a mixture of amyloid fibrils presumably from α-synuclein along with amorphous protein aggregate presumably from DJ-1. Electron microscopy analysis of DJ-1^{V51C} and α-synuclein showed very few aggregated particles and no fibrillar material (Figure 4b). The DJ-1^{V51C} and α-synuclein mixture upon SDS-PAGE analysis showed presence of both proteins and no degradation products suggesting both samples were stable over the course of the experiment (supplemental figure 1c).

Discussion

Since the discovery of parkin mutations, two additional genes have been found associated with recessive parkinsonism, DJ-1(2) and PINK1 (58–62). Patients with mutations in either of these two genes have similar phenotypes to each other and to parkin. Onset is generally early (from ages 30 to 50), and the course is benign with long disease duration. Individuals with DJ-1 mutations have loss of presynaptic dopaminergic function, although no autopsy studies are yet available. Most PD patients have either homozygous or compound heterozygous DJ-1 mutations, but some also have single heterozygous mutations, suggesting that DJ-1 loss-of-function accounts for disease in these individuals. The exact function of DJ-1 remains elusive, but evidence points towards functions similar to a free radical scavenger, or a redox dependent chaperone or both(23,63). The presence of Cys 106 at the dimer interface of the protein in a unique chemical environment composed of charged amino acids is reminiscent of peroxidases. Indeed, Cys 106 has been shown to be readily oxidized, which presumably causes translocation of the protein to the mitochondria, where it may exert a neuroprotective effect(27). The mutations such as L166P, A104T and M26I, when mapped on the crystal structure, are distant from Cys 106 but are located on secondary structural elements that make up the dimer interface and cause loss of function indirectly through a loss of structural stability(10). The L166P is a severely destabilizing mutation, which compromises the dimeric structure of DJ-1 almost completely. Other mutations such as A104T and M26I have lesser degree of destabilizing effect on the protein structure. We used MD simulations to address the early structural changes that might accompany the loss of function. While proline mutations such as L166P are generally considered helix-breakers, in certain cases, the overall effect of the mutation is dependent on position of the mutation in the helix and the surrounding residue(64,65). In a short simulation of 1000ps to probe early events, DJ-1^{WT} was found to be stable over the course of the simulation, while DJ-1^{L166P}, DJ-1^{A104T} and DJ-1^{M26I} were found to be less stable. Interestingly, the L166P mutation caused a mere kink in helix G but the motion was translated to the region between residues 38–70 (see Figure 1b). This observation is consistent with independent simulation studies

out by Daggett and co-workers, NMR studies carried out by Eliezer et al. (40) and X-ray and solvent mapping studies carried out by Ringe and co-workers(41). This region of the protein lies at the dimer interface and was found to be highly susceptible to unfolding in our simulations. Though essential dynamic calculations were not performed to obtain a detailed picture of the motion-translation from the mutation site to the region 38–70 of the protein, it was clear that the overall stability of the protein was dependent on the stability of this region. It may be argued that if the weak-links in a protein which are highly susceptible to mutations are identified, they may be reinforced to prevent downstream unfolding events.

In order to test whether stabilization of the 38–70 regions affects overall stability, the residue V51 was mutated to C51 in the L166P, A104T or M26I familial mutant background to generate a pair of symmetric disulfide bridges with C53 on the opposite subunit. Under oxidizing conditions, the double mutants DJ-$1^{A104T/V51C}$ and DJ-$1^{M26I/V51C}$ were found to be stabilized against thermal and chemical denaturation. DJ-1^{L166P} did not form a covalent dimer, which is consistent with the observations made by other researchers that the L166P mutation is deleterious to the structure. While DJ-1^{WT} exhibited the ability to scavenge hydroperoxide radicals and block aggregation of α-synuclein, DJ-1^{A104T} and DJ-1^{M26I} did not. This was presumably due to perturbations at the dimer interface that destroys the subtle arrangement of charged residues around Cys106 responsible for DJ-1 . The double mutants DJ-$1^{A104T/V51C}$ and DJ-$1^{M26I/V51C}$ showed increased ability to scavenge hydroperoxide radicals compared to their familial mutant counterparts and could effectively block the aggregation of α-synuclein, suggesting at least a partial restoration of the Cys106 environment. An interesting observation was that the disulfide mutation in the WT background (DJ-1^{V51C}) showed prolonged chaperone like effect and could block aggregation of α-synuclien for extended periods of time, while DJ-1^{WT} was effective only up to 80hrs. This is presumably due to the fact that any protein upon agitation unfolds leading to loss of function. Engineered disulfide bonds are known to make proteins more resilient to unfolding.

The strategy of native-state stabilization for protein misfolding disease has been shown to be generally applicable to a number of human cases such as TTR (familial amyloidosis)(66), SOD-1 (Lou Gehrig's disease or ALS)(38,39) and glucocerebrosidase (Gaucher's disease) (67). While familial DJ-1 mutants represent a small percentage of Parkinson's patients, it may be argued that stabilization of DJ-1^{WT} with small molecules may have beneficial effects in patients with various synucleinopathies due to potentiated chaperone-like function, which may increase neuroprotection. The results described in this investigation along with those in the current literature, in effect validate an extensive search for drug-like molecules that affect protein stability, analogous to those described in the case of TTR and SOD. Such molecules could eventually be developed into desperately needed therapeutics for Parkinson's disease.

Supplementary Material

Refer to Web version on PubMed Central for supplementary material.

Acknowledgments

We wish to thank Dr. Peter Lansbury (P.T.L) for research support and Dr. Gregory Cuny at the Laboratory for Drug Discovery in Neurodegeneration (LDDN) for useful discussions on assay design, small molecule screening and analysis of the hits. We wish to thank Prof. Jean-Christopher Rochet (Purdue University), John Hulleman (Purdue University) and Prof. Liang Tong (Columbia University) for providing the initial clones for human DJ-1. However, all work described in this manuscript was carried out using the clones synthesized at DNA2.0. We would like to thank Kristine Vernon for help with manuscript preparation.

‡This work was supported by the National Institutes of Health (AG08476 and NS038375 to P.T.L)

List of abbreviations

PD	Parkinson’s Disease
ROS	reactive oxygen species
TTR	Transthyretin
SOD	Human superoxide dismutase-1
GST	Glutathione-s-transferase
CCD	Charge couple detector
PBS	Phosphate buffer saline
MWCO	molecular weight cut-off
TBS	Tris. Buffer saline pH7.4

References

1. Dawson TM, Dawson VL. Molecular pathways of neurodegeneration in Parkinson's disease. Science. 2003; 302:819–822. [PubMed: 14593166]
2. Bonifati V, Rizzu P, van Baren MJ, Schaap O, Breedveld GJ, Krieger E, Dekker MC, Squitieri F, Ibanez P, Joosse M, van Dongen JW, Vanacore N, van Swieten JC, Brice A, Meco G, van Duijn CM, Oostra BA, Heutink P. Mutations in the DJ-1 gene associated with autosomal recessive early-onset parkinsonism. Science. 2003; 299:256–259. [PubMed: 12446870]
3. Macedo MG, Anar B, Bronner IF, Cannella M, Squitieri F, Bonifati V, Hoogeveen A, Heutink P, Rizzu P. The DJ-1 L166P mutant protein associated with early onset Parkinson's disease is unstable and forms higher-order protein complexes. Hum Mol Genet. 2003; 12:2807–2816. Epub 2003 Sep 2802. [PubMed: 12952867]
4. Miller DW, Ahmad R, Hague S, Baptista MJ, Canet-Aviles R, McLendon C, Carter DM, Zhu PP, Stadler J, Chandran J, Klinefelter GR, Blackstone C, Cookson MR. L166P mutant DJ-1, causative for recessive Parkinson's disease, is degraded through the ubiquitin-proteasome system. J Biol Chem. 2003; 278:36588–36595. Epub 32003 Jul 36588. [PubMed: 12851414]
5. Abou-Sleiman PM, Healy DG, Quinn N, Lees AJ, Wood NW. The role of pathogenic DJ-1 mutations in Parkinson's disease. Ann. Neurol. 2003; 54:283–286. [PubMed: 12953260]
6. Hering R, Strauss KM, Tao X, Bauer A, Woitalla D, Mietz EM, Petrovic S, Bauer P, Schaible W, Muller T, Schols L, Klein C, Berg D, Meyer PT, Schulz JB, Wollnik B, Tong L, Kruger R, Riess O. Novel homozygous p.E64D mutation in DJ1 in early onset Parkinson disease (PARK7). Hum. Mutat. 2004; 24:321–329. [PubMed: 15365989]
7. Annesi G, Savettieri G, Pugliese P, D'Amelio M, Tarantino P, Ragonese P, La Bella V, Piccoli T, Civitelli D, Annesi F, Fierro B, Piccoli F, Arabia G, Caracciolo M, Ciro Candiano IC, Quattrone A. DJ-1 mutations and parkinsonism-dementia-amyotrophic lateral sclerosis complex. Ann Neurol. 2005; 58:803–807. [PubMed: 16240358]
8. Hague S, Rogaeva E, Hernandez D, Gulick C, Singleton A, Hanson M, Johnson J, Weiser R, Gallardo M, Ravina B, Gwinn-Hardy K, Crawley A, St George-Hyslop PH, Lang AE, Heutink P, Bonifati V, Hardy J. Early-onset Parkinson's disease caused by a compound heterozygous DJ-1 mutation. Ann Neurol. 2003; 54:271–274. [PubMed: 12891685]
9. Clark LN, Afridi S, Mejia-Santana H, Harris J, Louis ED, Cote LJ, Andrews H, Singleton A, Wavrant De-Vrieze F, Hardy J, Mayeux R, Fahn S, Waters C, Ford B, Frucht S, Ottman R, Marder K. Analysis of an early-onset Parkinson's disease cohort for DJ-1 mutations. Mov Disord. 2004; 19:796–800. [PubMed: 15254937]
10. Lakshminarasimhan M, Maldonado MT, Zhou W, Fink AL, Wilson MA. Structural impact of three Parkinsonism-associated missense mutations on human DJ-1. Biochemistry. 2008; 47:1381–1392. [PubMed: 18181649]

11. Nagakubo D, Taira T, Kitaura H, Ikeda M, Tamai K, Iguchi-Ariga SM, Ariga H. DJ-1, a novel oncogene which transforms mouse NIH3T3 cells in cooperation with ras. Biochem Biophys Res Commun. 1997; 231:509–513. [PubMed: 9070310]
12. Klinefelter GR, Laskey JW, Ferrell J, Suarez JD, Roberts NL. Discriminant analysis indicates a single sperm protein (SP22) is predictive of fertility following exposure to epididymal toxicants. J Androl. 1997; 18:139–150. [PubMed: 9154508]
13. Aleyasin H, Rousseaux MW, Phillips M, Kim RH, Bland RJ, Callaghan S, Slack RS, During MJ, Mak TW, Park DS. The Parkinson's disease gene DJ-1 is also a key regulator of stroke-induced damage. Proc Natl Acad Sci U S A. 2007; 104:18748–18753. [PubMed: 18003894]
14. Shinbo Y, Taira T, Niki T, Iguchi-Ariga SM, Ariga H. DJ-1 restores p53 transcription activity inhibited by Topors/p53BP3. Int J Oncol. 2005; 26:641–648. [PubMed: 15703819]
15. Taira T, Iguchi-Ariga SM, Ariga H. Co-localization with DJ-1 is essential for the androgen receptor to exert its transcription activity that has been impaired by androgen antagonists. Biol Pharm Bull. 2004; 27:574–577. [PubMed: 15056870]
16. Takahashi K, Taira T, Niki T, Seino C, Iguchi-Ariga SM, Ariga H. DJ-1 positively regulates the androgen receptor by impairing the binding of PIASx alpha to the receptor. J Biol Chem. 2001; 276:37556–37563. [PubMed: 11477070]
17. Zhong N, Kim CY, Rizzu P, Geula C, Porter DR, Pothos EN, Squitieri F, Heutink P, Xu J. DJ-1 transcriptionally up-regulates the human tyrosine hydroxylase by inhibiting the sumoylation of pyrimidine tract-binding protein-associated splicing factor. J Biol Chem. 2006; 281:20940–20948. [PubMed: 16731528]
18. Hod Y, Pentyala SN, Whyard TC, El-Maghrabi MR. Identification and characterization of a novel protein that regulates RNA-protein interaction. J Cell Biochem. 1999; 72:435–444. [PubMed: 10022524]
19. Shinbo Y, Niki T, Taira T, Ooe H, Takahashi-Niki K, Maita C, Seino C, Iguchi-Ariga SM, Ariga H. Proper SUMO-1 conjugation is essential to DJ-1 to exert its full activities. Cell Death Differ. 2006; 13:96–108. [PubMed: 15976810]
20. Kim RH, Peters M, Jang Y, Shi W, Pintilie M, Fletcher GC, DeLuca C, Liepa J, Zhou L, Snow B, Binari RC, Manoukian AS, Bray MR, Liu FF, Tsao MS, Mak TW. DJ-1, a novel regulator of the tumor suppressor PTEN. Cancer Cell. 2005; 7:263–273. [PubMed: 15766664]
21. Batelli S, Albani D, Rametta R, Polito L, Prato F, Pesaresi M, Negro A, Forloni G. DJ-1 modulates alpha-synuclein aggregation state in a cellular model of oxidative stress: relevance for Parkinson's disease and involvement of HSP70. PLoS ONE. 2008; 3:e1884. [PubMed: 18382667]
22. Li HM, Niki T, Taira T, Iguchi-Ariga SM, Ariga H. Association of DJ-1 with chaperones and enhanced association and colocalization with mitochondrial Hsp70 by oxidative stress. Free Radic Res. 2005; 39:1091–1099. [PubMed: 16298734]
23. Zhou W, Zhu M, Wilson MA, Petsko GA, Fink AL. The oxidation state of DJ-1 regulates its chaperone activity toward alpha-synuclein. J Mol Biol. 2006; 356:1036–1048. [PubMed: 16403519]
24. Wei Y, Ringe D, Wilson MA, Ondrechen MJ. Identification of functional subclasses in the DJ-1 superfamily proteins. PLoS Comput Biol. 2007; 3:e10. [PubMed: 17257049]
25. Lee SJ, Kim SJ, Kim IK, Ko J, Jeong CS, Kim GH, Park C, Kang SO, Suh PG, Lee HS, Cha SS. Crystal structures of human DJ-1 and Escherichia coli Hsp31, which share an evolutionarily conserved domain. J Biol Chem. 2003; 278:44552–44559. Epub 42003 Aug 44525. [PubMed: 12939276]
26. Kinumi T, Kimata J, Taira T, Ariga H, Niki E. Cysteine-106 of DJ-1 is the most sensitive cysteine residue to hydrogen peroxide-mediated oxidation in vivo in human umbilical vein endothelial cells. Biochem Biophys Res Commun. 2004; 317:722–728. [PubMed: 15081400]
27. Canet-Aviles RM, Wilson MA, Miller DW, Ahmad R, McLendon C, Bandyopadhyay S, Baptista MJ, Ringe D, Petsko GA, Cookson MR. The Parkinson's disease protein DJ-1 is neuroprotective due to cysteine-sulfinic aciddriven mitochondrial localization. Proc Natl Acad Sci U S A. 2004; 101:9103–9108. [PubMed: 15181200]
28. Krebiehl G, Ruckerbauer S, Burbulla LF, Kieper N, Maurer B, Waak J, Wolburg H, Gizatullina Z, Gellerich FN, Woitalla D, Riess O, Kahle PJ, Proikas-Cezanne T, Kruger R. Reduced basal

autophagy and impaired mitochondrial dynamics due to loss of Parkinson's disease-associated protein DJ-1. PLoS One. 5:e9367. [PubMed: 20186336]

29. Scherz-Shouval R, Elazar Z. ROS, mitochondria and the regulation of autophagy. Trends Cell Biol. 2007; 17:422–427. [PubMed: 17804237]
30. Kim I, Rodriguez-Enriquez S, Lemasters JJ. Selective degradation of mitochondria by mitophagy. Arch Biochem Biophys. 2007; 462:245–253. [PubMed: 17475204]
31. Witt AC, Lakshminarasimhan M, Remington BC, Hasim S, Pozharski E, Wilson MA. Cysteine pKa depression by a protonated glutamic acid in human DJ-1. Biochemistry. 2008; 47:7430–7440. [PubMed: 18570440]
32. Wilson MA, Collins JL, Hod Y, Ringe D, Petsko GA. The 1.1-A resolution crystal structure of DJ-1, the protein mutated in autosomal recessive early onset Parkinson's disease. Proc Natl Acad Sci U S A. 2003; 100:9256–9261. [PubMed: 12855764]
33. Hulleman JD, Mirzaei H, Guigard E, Taylor KL, Ray SS, Kay CM, Regnier FE, Rochet JC. Destabilization of DJ-1 by familial substitution and oxidative modifications: implications for Parkinson's disease. Biochemistry. 2007; 46:5776–5789. [PubMed: 17451229]
34. Gorner K, Holtorf E, Waak J, Pham TT, Vogt-Weisenhorn DM, Wurst W, Haass C, Kahle PJ. Structural determinants of the C-terminal helix-kink-helix motif essential for protein stability and survival promoting activity of DJ-1. J Biol Chem. 2007; 282:13680–13691. [PubMed: 17331951]
35. Blackinton J, Ahmad R, Miller DW, van der Brug MP, Canet-Aviles RM, Hague SM, Kaleem M, Cookson MR. Effects of DJ-1 mutations and polymorphisms on protein stability and subcellular localization. Brain Res Mol Brain Res. 2005; 134:76–83. [PubMed: 15790532]
36. Moore DJ, Zhang L, Troncoso J, Lee MK, Hattori N, Mizuno Y, Dawson TM, Dawson VL. Association of DJ-1 and parkin mediated by pathogenic DJ-1 mutations and oxidative stress. Hum Mol Genet. 2005; 14:71–84. [PubMed: 15525661]
37. Adamski-Werner SL, Palaninathan SK, Sacchettini JC, Kelly JW. Diflunisal analogues stabilize the native state of transthyretin. Potent inhibition of amyloidogenesis. J Med Chem. 2004; 47:355–374. [PubMed: 14711308]
38. Ray SS, Nowak RJ, Strokovich K, Brown RH Jr, Walz T, Lansbury PT Jr. An intersubunit disulfide bond prevents in vitro aggregation of a superoxide dismutase-1 mutant linked to familial amytrophic lateral sclerosis. Biochemistry. 2004; 43:4899–4905. [PubMed: 15109247]
39. Ray SS, Nowak RJ, Brown RH Jr, Lansbury PT Jr. Small-molecule-mediated stabilization of familial amyotrophic lateral sclerosis-linked superoxide dismutase mutants against unfolding and aggregation. Proc Natl Acad Sci U S A. 2005; 102:3639–3644. [PubMed: 15738401]
40. Malgieri G, Eliezer D. Structural effects of Parkinson's disease linked DJ-1 mutations. Protein Sci. 2008; 17:855–868. [PubMed: 18436956]
41. Landon MR, Lieberman RL, Hoang QQ, Ju S, Caaveiro JM, Orwig SD, Kozakov D, Brenke R, Chuang GY, Beglov D, Vajda S, Petsko GA, Ringe D. Detection of ligand binding hot spots on protein surfaces via fragment-based methods: application to DJ-1 and glucocerebrosidase. J Comput Aided Mol Des. 2009:491–500.
42. Anderson PC, Daggett V. Molecular basis for the structural instability of human DJ-1 induced by the L166P mutation associated with Parkinson's disease. Biochemistry. 2008; 47:9380–9393. [PubMed: 18707128]
43. Van Der Spoel D, Lindahl E, Hess B, Groenhof G, Mark AE, Berendsen HJ. GROMACS: fast, flexible, and free. J Comput Chem. 2005; 26:1701–1718. [PubMed: 16211538]
44. Bjork A, Dalhus B, Mantzilas D, Eijsink VG, Sirevag R. Stabilization of a tetrameric malate dehydrogenase by introduction of a disulfide bridge at the dimer-dimer interface. J Mol Biol. 2003; 334:811–821. [PubMed: 14636605]
45. Zavialov A, Benndorf R, Ehrnsperger M, Zav'yalov V, Dudich I, Buchner J, Gaestel M. The effect of the intersubunit disulfide bond on the structural and functional properties of the small heat shock protein Hsp25. Int J Biol Macromol. 1998; 22:163–173. [PubMed: 9650071]
46. Gokhale RS, Ray SS, Balaram H, Balaram P. Unfolding of Plasmodium falciparum triosephosphate isomerase in urea and guanidinium chloride: evidence for a novel disulfide exchange reaction in a covalently cross-linked mutant. Biochemistry. 1999; 38:423–431. [PubMed: 9890925]

47. MacDonald JT, Purkiss AG, Smith MA, Evans P, Goodfellow JM, Slingsby C. Unfolding crystallins: the destabilizing role of a beta-hairpin cysteine in betaB2-crystallin by simulation and experiment. Protein Sci. 2005; 14:1282–1292. [PubMed: 15840832]
48. Tao X, Tong L. Crystal structure of human DJ-1, a protein associated with early onset Parkinson's disease. J Biol Chem. 2003; 278:31372–31379. [PubMed: 12761214]
49. Dombkowski AA. Disulfide by Design: a computational method for the rational design of disulfide bonds in proteins. Bioinformatics. 2003; 19:1852–1853. [PubMed: 14512360]
50. Ericsson UB, Hallberg BM, Detitta GT, Dekker N, Nordlund P. Thermofluor-based high-throughput stability optimization of proteins for structural studies. Anal Biochem. 2006; 357:289–298. [PubMed: 16962548]
51. Mezzasalma TM, Kranz JK, Chan W, Struble GT, Schalk-Hihi C, Deckman IC, Springer BA, Todd MJ. Enhancing recombinant protein quality and yield by protein stability profiling. J Biomol Screen. 2007; 12:418–428. [PubMed: 17438070]
52. Cummings MD, Farnum MA, Nelen MI. Universal screening methods and applications of ThermoFluor. J Biomol Screen. 2006; 11:854–863. [PubMed: 16943390]
53. Jacobson RH, Matsumura M, Faber HR, Matthews BW. Structure of a stabilizing disulfide bridge mutant that closes the active-site cleft of T4 lysozyme. Protein Sci. 1992; 1:46–57. [PubMed: 1304882]
54. Gokhale RS, Agarwalla S, Francis VS, Santi DV, Balaram P. Thermal stabilization of thymidylate synthase by engineering two disulfide bridges across the dimer interface. J Mol Biol. 1994; 235:89–94. [PubMed: 7904654]
55. Velanker SS, Gokhale RS, Ray SS, Gopal B, Parthasarathy S, Santi DV, Balaram P, Murthy MR. Disulfide engineering at the dimer interface of Lactobacillus casei thymidylate synthase: crystal structure of the T155C/E188C/C244T mutant. Protein Sci. 1999; 8:930–933. [PubMed: 10211840]
56. Conway KA, Harper JD, Lansbury PT Jr. Fibrils formed in vitro from alpha-synuclein and two mutant forms linked to Parkinson's disease are typical amyloid. Biochemistry. 2000; 39:2552–2563. [PubMed: 10704204]
57. Caughey B, Lansbury PT. Protofibrils, pores, fibrils, and neurodegeneration: separating the responsible protein aggregates from the innocent bystanders. Annu Rev Neurosci. 2003; 26:267–298. [PubMed: 12704221]
58. Yang YX, Wood NW, Latchman DS. Molecular basis of Parkinson's disease. Neuroreport. 2009; 20:150–156. [PubMed: 19151598]
59. Biskup S, Gerlach M, Kupsch A, Reichmann H, Riederer P, Vieregge P, Wullner U, Gasser T. Genes associated with Parkinson syndrome. J Neurol. 2008; 255 Suppl 5:8–17. [PubMed: 18787878]
60. Bonifati V. Genetics of parkinsonism. Parkinsonism Relat Disord. 2007; 13 Suppl 3:S233–S241. [PubMed: 18267242]
61. da Costa CA. DJ-1: a newcomer in Parkinson's disease pathology. Curr Mol Med. 2007; 7:650–657. [PubMed: 18045143]
62. Dodson MW, Guo M. Pink1, Parkin, DJ-1 and mitochondrial dysfunction in Parkinson's disease. Curr Opin Neurobiol. 2007; 17:331–337. [PubMed: 17499497]
63. Shendelman S, Jonason A, Martinat C, Leete T, Abeliovich A. DJ-1 is a redox-dependent molecular chaperone that inhibits alpha-synuclein aggregate formation. PLoS Biol. 2004; 2:e362. [PubMed: 15502874]
64. Li SC, Goto NK, Williams KA, Deber CM. Alpha-helical, but not beta-sheet, propensity of proline is determined by peptide environment. Proc Natl Acad Sci U S A. 1996; 93:6676–6681. [PubMed: 8692877]
65. Chakrabarti P, Chakrabarti S. C--H…O hydrogen bond involving proline residues in alpha-helices. J Mol Biol. 1998; 284:867–873. [PubMed: 9837710]
66. Hammarstrom P, Wiseman RL, Powers ET, Kelly JW. Prevention of transthyretin amyloid disease by changing protein misfolding energetics. Science. 2003; 299:713–716. [PubMed: 12560553]
67. Lieberman RL, Wustman BA, Huertas P, Powe AC Jr, Pine CW, Khanna R, Schlossmacher MG, Ringe D, Petsko GA. Structure of acid beta-glucosidase with pharmacological chaperone provides insight into Gaucher disease. Nat Chem Biol. 2007; 3:101–107. [PubMed: 17187079]

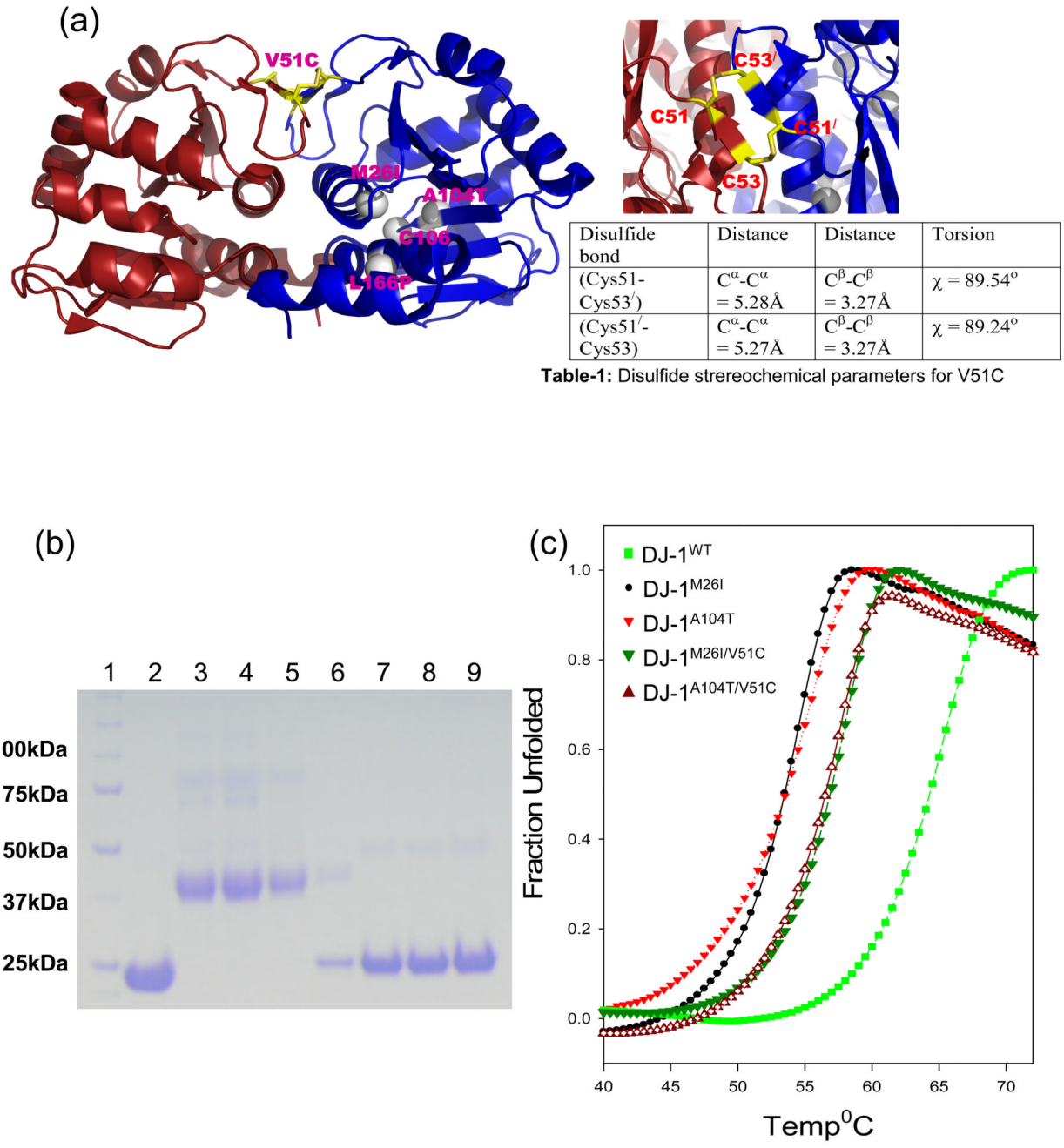

Disulfide bond	Distance	Distance	Torsion
(Cys51-Cys53′)	C^{α}-C^{α} = 5.28Å	C^{β}-C^{β} = 3.27Å	$\chi = 89.54^{o}$
(Cys51′-Cys53)	C^{α}-C^{α} = 5.27Å	C^{β}-C^{β} = 3.27Å	$\chi = 89.24^{o}$

Table-1: Disulfide strereochemical parameters for V51C

Figure 1.

(a) Ribbon representation of the two subunits of DJ-1 showing the positions of the various familial Parkinson's disease causing mutations and the disulfide linkages (side panel) used in this investigation. Table -1 shows the stereochemical parameters for the disulfide bonds generated as a result of V51C mutation. (b) 4–12% gradient SDS-PAGE analysis of disulfide bond formation in DJ-1^{V51C}, DJ-$1^{L166P/V51C}$, DJ-$1^{M26I/V51C}$ and DJ-$1^{V51C/A104T}$ under non-reducing conditions. The lanes are as follows: Lane 1 is molecular weight marker and Lane 2 is DJ-1^{WT}. Lanes 3–6 are DJ-1^{V51C}, DJ-$1^{M26I/V51C}$, DJ-$1^{A104T/V51C}$ and DJ-$1^{L166P/V51C}$ respectively under non-reducing conditions. Lanes 7–9 are DJ-1^{V51C}, DJ-$1^{M26I/V51C}$ and DJ-$1^{A104T/V51C}$ under reducing conditions. (c) Thermal melting curves

(fluorescence) for DJ-1^{WT} and various mutants measured using thermofluor (sypro orange) on a realtime PCR machine. Thermal melting curves for each protein sample was measured from three independent wells (*n*=3) and the averaged data is shown here. The melting curves indicate that the DJ-1^{WT} is the most stable with Tm=65±0.5°C. The familial mutants were found to be less stable than WT with DJ-1^{M26I} (Tm=52±0.5°C) and DJ-1^{A104T}(Tm=53±0.5°C). The V51C disulfide-linked versions of the mutant DJ-1 were more stable compared to the familial mutants (DJ-$1^{M26I/V51C}$ Tm=57±0.5°C, DJ-$1^{A104T/V51C}$ Tm=58±0.5°C)

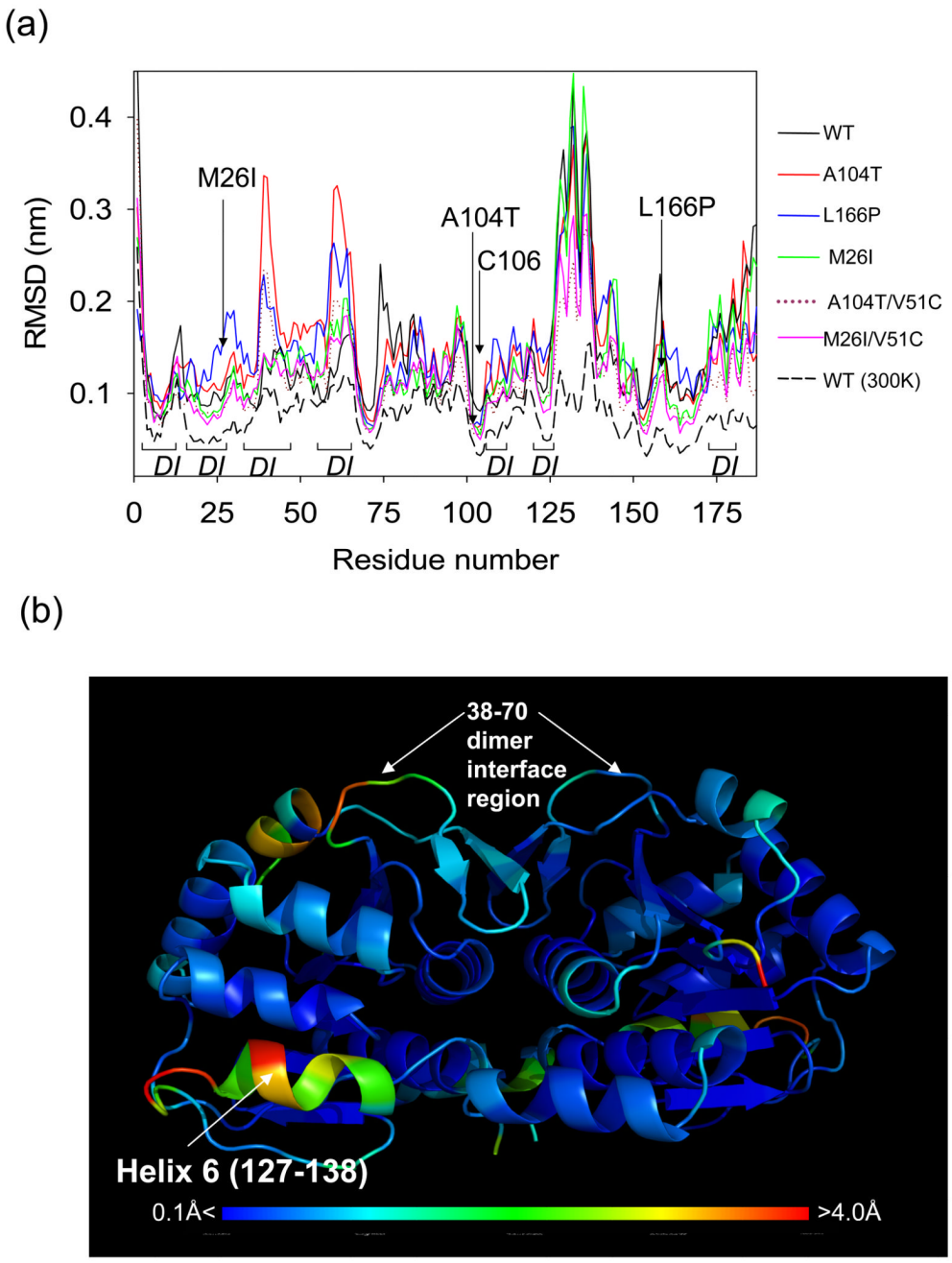

Figure 2.

(a) R.M.S deviation per residue for the Cα atom for DJ-1^{WT}, the familial Parkinson's disease mutants and their disulfide versions DJ-1$^{M26I/V51C}$ and DJ-1$^{A104T/V51C}$ observed over the course of 1000ps MD simulation. The maximum variability between WT and the various mutants is observed between residues 38 and 70, parts of which coincide with the dimer interface and include the V51 region. Other region of the protein with high mobility includes the solvent exposed helix 6 between residues 127–138. Key residues important in this investigation and indicated by arrows and the dimer interface residues are indicated by *DI*. Among the mutants DJ-1^{A104T} and DJ-1^{L166P} appear to have more perturbation compared to DJ-1^{M26I} around the 38–70 region. Simulation trajectories of the disulfide

bonded counterparts of these mutants are indicated by brown dotted line (DJ-$1^{A104T/V51C}$) and pink line (DJ-$1^{M26I/V51C}$). (b) Ribbon representation of DJ-1^{A104T} representing the molecular motions in the various parts of the protein. The per-residue R.M.S variation of figure 2a was converted to B-factors and ramped using the coloring scheme indicated below (blue; R.MS.D = 0.0 Å, red; R.M.S.D = 4.0 Å). Two mobile regions including the dimer interface residues (38–70) and helix 6 (127–138) are indicated by arrows.

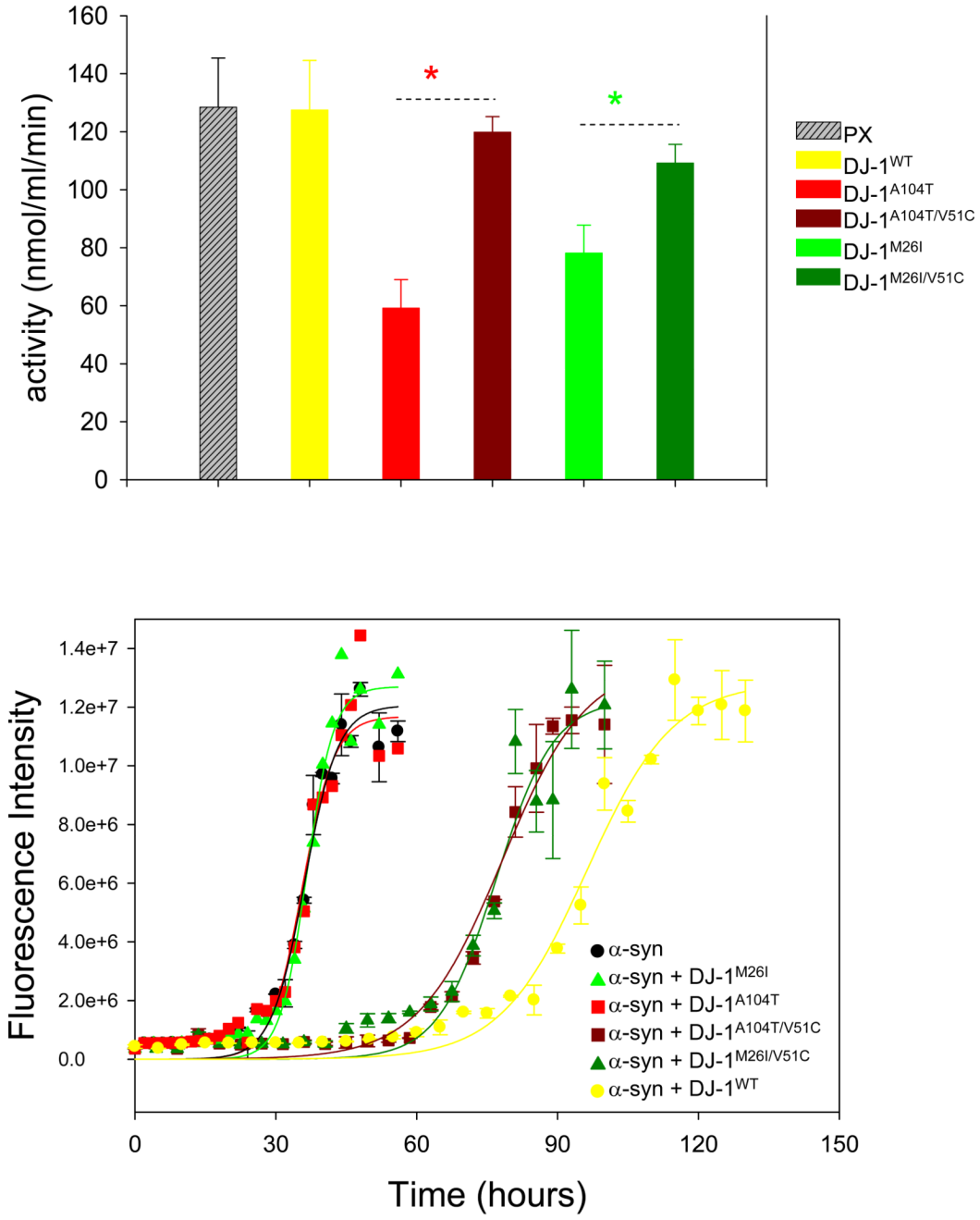

Figure 3.

(a) Autooxidation of Cys 106 of DJ-1^{WT}, familial mutants and disulfide bonded (V51C) versions of the familial mutants are compared using a glutathione-peroxidase (PX) assay kit. 100nM of glutathione peroxidase (PX) was used as a positive control in this assay. The disulfide mutant DJ-1$^{A104T/V51C}$ showed increased ability to autooxidize compared to DJ-1^{A104T} (n=5, *, p<0.0001 Student's t-test). Similarly, DJ-1$^{M26I/V51C}$ showed higher glutathione peroxidase activity as compared to DJ-1^{M26I} (n=5, *, p=0.0004 Student's t-test). (b) Aggregation of α-synuclein in presence of various DJ-1^{WT} and various mutants. Data from five independent aggregation experiments for α-synuclein incubated various forms of DJ-1 was used for generation of the plot and error bars. α-synuclein aggregates to

completion within 48hrs under our assay conditions. The mutants DJ-1^{A104T} and DJ-1^{M26I} have no effect on α-synuclein aggregation kinetics. DJ-1^{WT} delays the aggregation of α-synuclein with the first Thio-T positive aggregates appearing around 80hrs. The V51C disulfide bonded mutants DJ-1$^{A104T/V51C}$ and DJ-1$^{A104T/V51C}$ delays the aggregation of α-synuclein with the first Thio-T positive aggregates appearing after 60hrs.

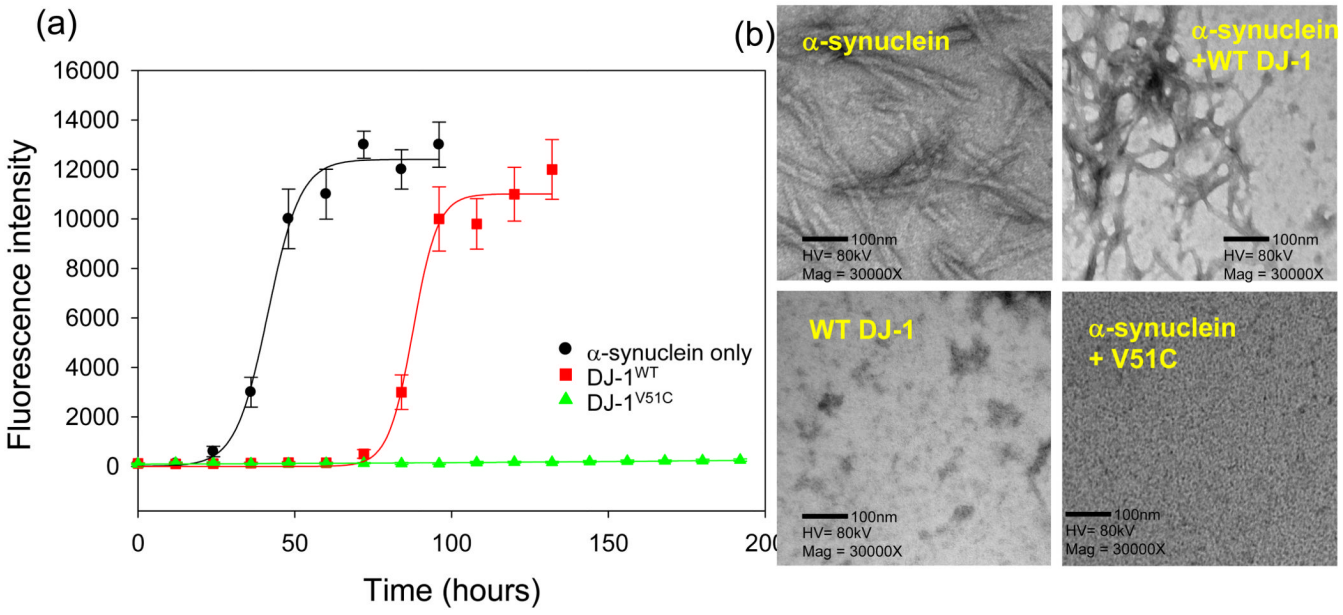

Figure 4.

Aggregation of α-synuclein in presence of DJ-1^{WT} and DJ-1^{V51C} followed over extended periods of time. DJ-1^{WT} is effective in blocking aggregation; however the effects lasts only till 80hrs (First thio-T positive aggregates observed after 80hrs). The disulfide bonded DJ-1^{V51C} can exert its anti-aggregation effects for longer periods of time beyond 80hrs. In this experiment, the aggregation kinetics was followed up to 196hrs during which no aggregation of α-synuclein was observed. Data from five independent aggregation assays were used to generate the plot and error bars in this study (b) Electron microscopy analysis of mixtures of DJ-1^{WT}+α-synuclein and DJ-1^{V51C}+α-synuclein after 80hrs of incubation (representative electron microscopy field shown here at 30000×). The DJ-1^{WT}+α-synuclein mixture shows both fibrillar aggregates as well as amorphous aggregates. Analysis of pure samples of α-synuclein in the control experiments shows fibrillar aggregates with amyloid like characteristic, while DJ-1^{WT} shows amorphous aggregates.